Metabolic and pathological effects of temporal lobe epilepsy in rat brain detected by proton spectroscopy and imaging

Takaaki Tokumitsu[a,1], **Anthony Mancuso**[b], **Philip R. Weinstein**[b], **Michael W. Weiner**[a,c], **Shoji Naruse**[d], and **Andrew A. Maudsley**[a,*]

[a] Department of Radiology, University of California San Francisco, Magnetic Resonance Unit 114M, Department of Veterans Affairs Medical Center, 4150 Clement Street, San Francisco, CA 94121, USA

[b] Department of Neurosurgery, University of California San Francisco, Magnetic Resonance Unit 114M, Department of Veterans Affairs Medical Center, 4150 Clement Street, San Francisco, CA 94121, USA

[c] Department of Medicine, University of California San Francisco, Magnetic Resonance Unit 114M, Department of Veterans Affairs Medical Center, 4150 Clement Street, San Francisco, CA 94121, USA

[d] Department of Neurosurgery, Kyoto Prefectural University of Medicine, Kawaramachi Hirokoji, Kamigyo-ku, Kyoto 602, Japan

Abstract

The goal of these experiments was to test the hypothesis that in an animal model of temporal lobe epilepsy (TLE), magnetic resonance spectroscopic measurement of *N*-acetylaspartate (NAA) and other metabolites, together with magnetic resonance imaging, provides a sensitive in vivo method to localize and monitor the progression of neuronal cell death and gliosis. Seizures were induced in rats by unilateral hippocampal injection of kainate. Magnetic resonance measurements were made from 1 to 84 days using proton spectroscopic imaging (^{1}H-MRSI), T2-weighted imaging (T2WI) and diffusion-weighted imaging (DWI). The results were compared with findings on histological sections. Decreased NAA and creatine levels and increased apparent diffusion coefficient of water were found in the ipsilateral hippocampus after 14 days where neuronal loss and gliosis were observed. In the contralateral hippocampus a significant increase of choline level was observed. These results suggest that ^{1}H-MRSI is a useful in vivo method for localizing neuronal loss and may also indicate additional pathological and metabolic alterations. In addition, DWI may be a useful method for in vivo detection of tissue alterations due to TLE.

Keywords

Magnetic resonance spectroscopic imaging; Diffusion-weighted imaging; *N*-Acetylaspartate; Creatine; Choline; Rat brain; Kainate; Epilepsy

* Corresponding author. Fax: (1) (415) 668-2864..
[1]Present address: Department of Neurosurgery, Kyoto Prefectural University of Medicine, Kyoto, Japan.

1. Introduction

A distinctive pathological feature of clinical temporal lobe epilepsy (TLE) is mesial temporal sclerosis characterized by neuronal loss and gliosis, though it is unclear whether this morphological change is a cause or a consequence of TLE [16]. These changes associated with mesial temporal lobe sclerosis may be identified using magnetic resonance imaging (MRI), which shows atrophy in the affected region [51] and hyperintensity in T2-weighted images [22,26]. Proton magnetic resonance spectroscopy and spectroscopic imaging (^{1}H-MRSI) have also been used to identify the epileptogenic focus by detection of neuronal cell loss in unilateral or bilateral hippocampi as indicated by reduction of *N*-acetylaspartate (NAA) [8,10,18,21]. To identify the affected region, different indices based on metabolite signal intensities have been proposed, including ratios of NAA/creatine [8] or NAA/(choline + creatine) [10,18].

Animal studies of epilepsy have been performed by administration of the seizure inducing drug kainate. Detection of mesial temporal sclerosis by MRI has been reported in animal models, including T2-weighted MRI and diffusion-weighted MRI in the rat [24,39,46]. These MRI techniques mainly indicate edema in the acute stage or gliosis in the chronic stage and it is difficult to confirm neuronal cell loss directly [15]. A reduction of NAA that correlated with neuronal loss, has been shown in the limbic system of the rat using ^{1}H-MRSI following systemic injection of kainate [15]. However, this animal model results in lesions occurring symmetrically in the limbic system [5], which makes it unsuitable for investigating unilateral temporal lobe epilepsy where asymmetric lesions are most commonly found [2,31,48]. A focal epilepsy animal model can be produced by unilateral injection of an epileptogenic substance into the limbic structure, which results in a single seizure focus. Focal administration of kainate in the corpus striatum has been used as such a model, which has been studied using spectroscopic imaging in rats [19]. However, since the corpus striatum is in the basal ganglia, kainate injection in this region does not provide a good model of TLE which usually arises from limbic structures. More suitable sites for injection are the amygdala [4], hippocampus [49] and deep prepiriform cortex [42]. Injection into the posterior hippocampus [12,13] appears to be suitable for modeling human temporal lobe epilepsy where sclerosis occurs mainly in the anterior hippocampus [3], since this region in the rat is homologous to the anterior hippocampus in humans [12].

The morphological changes which occur after kainate injection are neuronal cell death followed by gliosis [38,52] and mossy fiber reorganization [11,32,37,55]. Each of these pathological effects may result in observable changes seen with one or more magnetic resonance techniques. The aims of this study were to determine: (1) whether proton spectroscopic imaging (^{1}H-MRSI), T2-weighted imaging (T2WI) and diffusion-weighted imaging (DWI) show changes in the acute and chronic stages following focal administration of kainate; (2) to monitor the time course of changes in NAA, creatine and choline with ^{1}H-MRSI and MRI observed intensities on T2-weighted, diffusion-weighted and apparent diffusion coefficient (ADC) images; and (3) which of these indicators is most sensitive for detection of neuronal cell loss. These aims are accomplished by performing nuclear magnetic resonance (NMR) measurements at intervals from 1 day to 84 days following focal administration of kainate in the rat.

2. Materials and methods

2.1. Animal preparation

Male Sprague-Dawley rats (270–300 g) were anesthetized by inhalation of 4% isoflurane, intubated endotracheally and ventilated using 1.8–2.0% isoflurane with a mixture of oxygen and nitrous oxide. Atropine sulfate (0.33 mg/kg i.p). was used to reduce salivation and tracheal secretion. A burr hole was drilled in the skull 5.8 mm posterior to and 4.8 mm lateral of the

bregma. Seizure was induced by stereotaxic injection of 1.0 μg kainic acid (Sigma Chemical Co., St. Louis, MO) dissolved in 0.2 μl normal saline, into the left posterior hippocampus at a depth of 5.0 mm ventral to the brain surface [41]. The burr hole was then filled with bone cement to avoid leakage of cerebrospinal fluid. The duration for the injection was 5 min, which ensured good localization for the kainate administration while minimizing the time required for anesthesia. The total time of anesthesia and surgery was about 30 min, with onset of status epilepticus typically occurring within 60 min following kainate administration. Rats that did not demonstrate seizure behavior were excluded from the study. In order to control for effects of the surgery, a group of sham control animals were operated in an identical manner and they received an injection of 0.2 μl saline. Results obtained on these animals were also compared to a group of control animals not subjected to surgery.

T2WI, DWI and ^{1}H-MRSI were performed on seven groups of six kainate-injected rats, at times of 1, 3, 7, 14, 28, 56 and 84 days after injection. In addition, six unoperated rats (time point 0) and six sham control rats at both 3 and 28 days after saline injection were also examined, for a total of 60 rats in this study. For the NMR measurements the animals were anesthetized in the same manner as previously described. Polyethylene catheters were placed in a femoral artery and a femoral vein for monitoring blood gases (paCO$_2$, paO$_2$), pH and blood pressure, as well as for intravenous administration of pharmacological agents. Blood samples were obtained near the start and end of NMR measurements. Pancuronium bromide (0.33 mg/ kg) was administered every hour during anesthesia to minimize animal motion. Body temperature was monitored using a rectal thermometer and maintained at 36°C by circulating warm air through the bore of the magnet.

2.2. NMR methods

Experiments were performed at 7 Tesla (300 MHz proton resonance frequency) using a QUEST 4400 imaging spectrometer (Nalorac, Martinez, CA, USA). Rats were positioned in the magnet in a prone position, with the ears used as landmarks to place the bregma in the center of the magnet and at the center of an oval surface coil (2.5 × 3.0 cm) that was placed close to the dorsal surface of the head. This coil was used for both radio frequency excitation and reception in all measurements. Positioning of the animal was confirmed using T2-weighted MRI. Water suppressed, three dimensional ^{1}H-MRSI [17] was performed with spin echo observation at an echo time (TE) of 272 ms and a repetition time (TR) of 1 s. B1-compensated adiabatic excitation and refocusing pulses were used, with a 45° excitation pulse angle. Data was acquired with 16 × 16 × 20 phase encodings, a signal average of two and a field of view (FOV) of 3.5 × 3.5 × 4.0 cm^3. Data were collected as symmetrical echoes with 512 points and spectral width of 2000 Hz.

Multiplane T2WI and DWI were obtained with TE = 80 ms and TR = 1000 ms. The slice thickness was 2 mm and slice selection was set to correspond with coronal slices of the 3-dimensional ^{1}H-MRSI. A 128 × 128 acquisition matrix was obtained over a 3.5 × 3.5 cm^2 FOV and was zero-filled to 256 × 256 for display. For diffusion weighting, two 10 ms gradient pulses were applied along the long axis of the brain before and after the 180° pulse, for a diffusion attenuation or 'b' value of 1590 s/mm^2.

2.3. Data processing

For the ^{1}H-MRSI data in the spectral domain, a Gaussian line broadening of 5 Hz was applied and the data were zero-filled to 1024 points before Fourier transformation. In the spatial domains the data were zero-filled to 32 × 32 × 20 points and mild Gaussian smoothing (corresponding to exp$^{-0.4}$ at the edges of k-space) was applied. After Fourier transformation, the data were examined with in-house software [33] and spectroscopic images for each metabolite were created by spectral integration over user-defined regions (e.g. from 1.9 to 2.1

ppm for NAA). Co-registration of T2WI and ^{1}H-MRSI data sets was confirmed by superposition of T2WI edge information on the spectroscopic images. The T2-weighted images were then used to identify regions of interest (ROIs), from which individual spectra were selected for further analysis. These spectra were then analyzed with an automatic curve-fitting procedure [60] with a Gaussian line-shape model, to obtain signal integrals for NAA, choline containing compounds (Cho), creatine + phosphocreatine (Cr) and lactate resonances.

Single voxel spectra, corresponding to a nominal tissue volume of $2.2 \times 2.2 \times 2.0$ mm^3, were selected from 7 ROIs: contralateral frontal cortex, bilateral amygdalae, bilateral anterior dorsal hippocampi and bilateral posterior dorsal hippocampi (Fig. 1). Due to the placement of the animal within the magnet, the selected slices containing the ROIs corresponded to 0, 2, 4 and 6 mm posterior to the bregma. The ROI in the posterior hippocampus was chosen to avoid the needle tract, which may exhibit changes due to damage surrounding the path of entry; accordingly, the selected region included part of the dentate gyrus. The ROI in anterior hippocampus also included the dentate gyrus due to the small size of the anterior dorsal hippocampus. The T2-weighted and diffusion-weighted image intensity values were also recorded for the same seven ROIs.

The measured metabolite integrals and MRI intensity values were normalized for each animal by comparison with the corresponding value obtained in the contralateral frontal cortex, where no tissue damage is expected, to provide indices of %NAA, %Cho, %Cr, %T2WI and %DWI. For example, %NAA in a ROI was calculated as:

$$\%NAA = 100 \cdot \frac{NAA_{ROI}}{NAA_{Frontal}}$$

(1)

where NAA_{ROI} is the NAA integral in the ROI and $NAA_{Frontal}$ is the NAA integral in contralateral frontal cortex. This normalization procedure assumes that the B1 inhomogeneity distribution over the selected ROI's is constant for all experiments. This was tested by performing several studies of a homogeneous fluid-filled phantom, which showed no significant differences between ipsilateral and contralateral ROI's for regions selected in the animal studies. For the animal studies, positioning of the rat head in the mounting assembly and placement of the surface coil was found to be quite reproducible. Moreover, the use of a relatively large surface coil and B1 compensated excitation pulses helped to minimize any spatial variation of signal intensity.

In addition to the above parameters, the apparent diffusion coefficient (ADC) was calculated by the equation:

$$ADC = \ln(S_0/S_n)/b$$

(2)

where S_n is the intensity of the diffusion-weighted image, S_0 is the intensity of the T2-weighted image and b is the diffusion gradient attenuation factor [27]. ADC values are shown in addition to DWI since they do not include the effects of T2 weighting. ADC maps were calculated using software developed in this laboratory [30], which reported average ADC values for ROIs corresponding to MRSI ROIs.

2.4. Histological analysis

At the end of MR measurements, 30 rats (three from each group) were perfused transcardially with a buffered 4% paraformaldehyde solution. The brains were removed and kept in the paraformaldehyde solution for several weeks, before being cut into 2-mm coronal slices and

embedded in paraffin. The location of the slices was chosen to correspond to the T2WI slices, using the bregma as a landmark. The embedded samples were then cut into 6-μm-thick sections which were stained with cresyl violet for assessment of neuronal loss and with hematoxylin–eosin (H-E) for confirmation of gliosis. A blinded observer evaluated neuronal loss by using the grading score as described by Pulsinelli [44], where grade 0 indicated normal, grade 1 indicated a few damaged neurons, grade 2 indicated many damaged neurons and grade 3 indicated extensive neuronal damage. The tissue areas used for histological evaluation were at the same location and of approximately the same size as the ROIs used for MR analysis.

2.5. Statistical analysis

All data are presented as mean±standard error. Normality of data in each group was tested by normal probability plotting. *F*-test and Bartlett's test were performed to confirm the equality of variance. The comparison of results for each ROI between normal controls and sham controls was done with two tailed unpaired *t*-test. The ANOVA test and two-tailed Dunnett's test were applied for comparisons between the initial and later time points. Analyses comparing physiological data at the start and end of MR acquisition were done with two-tailed unpaired *t*-test to confirm stability of the animal preparation. The correlations between histological data and data from MR measurements in each ROI were analyzed with Spearman's rank coefficient. The level of significance was set as $P<0.05$ in all analyses.

3. Results

3.1. Behavior and physiological data

All kainate treated rats included in this study showed severe limbic seizures, equivalent to class IV or V [45], for at least 3 h after awaking from anesthesia. Behavior included 'wet dog' shakes, myoclonus of the facial muscles followed by head nodding, rearing, falling and rotation [4, 49]. At the 28 and 56 day time period, some rats presented recurrent seizure activity [7] for about 1 min, which was triggered by handling before the NMR measurements.

Physiological variables at the start of measurement were as follows: maximum and minimum blood pressures were 125±7 mmHg and 85±5 mmHg; pH of arterial blood was 7.38±0.07; $p\mathrm{CO}_2$ was 32±6 mmHg; and $p\mathrm{O}_2$ was 141±37 mmHg. At the end of measurement, maximum and minimum of blood pressure were 122±9 mmHg and 83±8 mmHg; pH of arterial blood was 7.36±0.05; $p\mathrm{CO}_2$ was 34±5 mmHg; and $p\mathrm{O}_2$ was 143±31 mmHg. Abnormal physiological values were not observed and no significant changes were observed over time during the NMR measurements.

3.2. NMR measurements

Fig. 2 shows a T2-weighted MRI, an NAA image and a diffusion-weighted image for the same slice, obtained at 0 and 28 days following kainate injection. A small reduction in the NAA image intensity was consistently observed in the ipsilateral posterior hippocampus at day 28. A hypointensity of the ipsilateral hippocampus near the injection site was also observed on the diffusion-weighted image at day 28 (data not shown.)

The mean values at each time point for %NAA, %Cr, %Cho, %T2WI, %DWI and ADC in anterior and posterior hippocampi are plotted on Fig. 3 and Fig. 4. Significant changes compared with pre-kainate values are indicated by an asterisk. Results for the amygdalae are not included since no changes for any measured parameter were observed in this region. Kainate administration was associated with progressive and significant decreases of %NAA in the ipsilateral anterior hippocampus (significant at 84 days) and posterior hippocampus (significant from 3 days to 84 days) and %Cr in the ipsilateral posterior hippocampus (from 7 days to 84 days), with both reaching a minimum at approximately 14 days. A significant

increase of %Cho was found in the contralateral hippocampus, which tended to increase steadily over the whole period of the study. In addition, the ADC of ipsilateral posterior hippocampus increased 14 days post-injection.

The %DWI increased and ADC decreased (compared to pre-kainate values) in the ipsilateral posterior hippocampus 1 day after injection, though the changes were not significant. %T2WI showed no significant changes at any time points. There were also no significant differences between the unoperated group and the sham-operated group.

3.3. Histological examination

Typical pathological features in the chronic period are shown in Fig. 5. Neuronal loss was most obvious in the ipsilateral posterior hippocampus of kainate-treated rats, with one animal found to have grade 1, twelve with grade 2 and eight with grade 3 damage in this region. The ipsilateral anterior hippocampus was also affected, though to a lesser degree. In CA3 and CA4 pyramidal cells, neuronal loss was seen even at 1 day after kainate injection, with the severity increasing for up to 7 days. Gliosis was observed after 3 days and atrophy of the ipsilateral hippocampus became markedly evident by 28 days. In the ipsilateral amygdala, five rats showed grade 3 neuronal loss. In all contralateral ROIs including contralateral frontal cortex, no neuronal cell loss or gliosis were observed. In the sham control rats, a slight scar was seen at the site of the needle tract, near the CA3 neurons of ipsilateral posterior hippocampus, but no neuronal loss was found in any regions.

Calculation of correlation coefficients for histological grading score versus MR results showed a strong correlation between neuronal loss and (1) %NAA in the ipsilateral anterior hippocampus ($\rho=-0.68$, $P=0.0002$) and posterior hippocampus ($\rho=-0.77$, $P<0.0001$), (2) %Cr in the ipsilateral posterior hippocampus ($\rho=-0.726$, $P<0.0001$), and (3) ADC in the ipsilateral posterior hippocampus ($\rho=0.769$, $P<0.0001$.

4. Discussion

The major findings of this study were that: (1) the indices for NAA and Cr signals progressively decreased in ipsilateral hippocampus for a period of 14 days, with no changes of these resonances observed in contralateral regions; (2) the index for Cho increased in contralateral posterior hippocampus; (3) ADC increased in the ipsilateral posterior hippocampus; and (4) no significant changes were observed with T2WI.

4.1. Changes of NAA

NAA is an abundant amino acid in the mammalian central nervous system [54]. It has been reported to be specifically localized to neuronal cells [25,50] though its role is still not fully understood [6]. MR studies indicate that there is a good correlation between NAA signal intensity and neuronal cell loss as a result of ischemia [20] and kainate injection [15]. Several clinical studies of temporal lobe epilepsy [8,10,18,21] have indicated that a region of reduced NAA corresponds to the epileptogenic focus, where mesial temporal sclerosis exists. However, sclerosis in both temporal lobes is also observed [2,31,48], in which case lateralization of the NAA distribution becomes impossible [10].

In the rat brain there are direct inter-hippocampal connections [1], so that a unilaterally occurring excitation also involves the contralateral limbic structures. For example, injection of excitotoxin in the CA3 region of the anterior dorsal hippocampus produces neuronal cell loss in the contralateral hippocampus [7,29]. In this study, however, while five cases showed evidence of a lesion in the ipsilateral amygdala, no changes of NAA were found in the contralateral hippocampus, nor was any evidence of neuronal cell loss seen in this region on

histological assessment. This result is in agreement with the report of Davenport et al. [12] who concluded that the residual effects of anesthesia was responsible for minimizing the acute excitatory damage in the contralateral region [28]. However, in this study the period of anesthesia was relatively brief, being induced by inhalation of isoflurane, whereas in the study of Davenport it was sustained for a longer period by intraperitoneal injection of sodium pentobarbital and chloral hydrate.

An alternative explanation for the absence of contralateral lesions in this study is that the mechanisms for inhibition of excitation were diminished in ipsilateral hippocampus due to the effect of kainate on inhibitory neurons, such as GABAergic neurons. However, it has been reported that the density of GABAergic neurons in the area of pyramidal cell loss did not change in this animal model [12]. While this study does not identify the reason for absence of contralateral hippocampal injury, the side of NAA depletion was concordant with the side of kainate injection and this animal model is therefore useful for imitating lateralized mesial temporal sclerosis in humans.

In this study, a good correlation between the reduction of NAA and neuronal loss was found, with no recovery of NAA. Therefore, our results suggest progressive or delayed neuronal loss in this rat seizure model.

4.2. Changes of creatine and choline

In studies of human temporal lobe epilepsy differing findings of Cr and Cho changes have been reported. In two reports, an increase in ipsilateral Cr and Cho was found [10,18] which was suggested to indicate gliosis, since these same changes are found in cultured glia [56]. However, in another report [9,14] decreased Cr and no change of Cho in ipsilateral temporal lobe was reported, which is concordant with our results. A possible mechanism for this finding is that the increased Cr and Cho by gliosis was offset by the decreased signal due to neuronal loss, resulting in little change.

The only significant change found in the contralateral hippocampus was increased Cho signal. It is possible that this indicates gliosis in the absence of neuronal cell loss, perhaps as a result of the surgery [36]. However, sham controls did not indicate any changes in this region, nor was histological evidence of gliosis found. A more likely explanation for the increased Cho signal is that this may indicate increased membrane synthesis due to mossy fiber reorganization. The 3.2 ppm resonance observed with ^{1}H-NMR spectroscopy reflects total choline stores, including precursors of phosphatidylcholine, which is the main component of cell membranes [35]. Large quantities of choline and choline-containing metabolites may be necessary for axonal regeneration. Furthermore, lipids such as phosphatidylcholine are produced in axons [57,58]. Sprouting of mossy fibers in the molecular layer of dentate gyrus has been described as a morphological change occurring 2 to 3 weeks after kainate treatment [11,32,37,55], and Davenport et al. [13] have reported that unilateral posterior hippocampal kainate injection produced sprouting of GABAergic and mossy fiber axons not only ipsilaterally but also contralaterally, where neuronal loss was absent. Tauck and Nadler [55] have reported that sprouted mossy fibers formed connections between granule cells which make a functional recurrent excitatory circuit. It is interesting to note that in a follow-up study of patients following removal of the epileptogenic focus, a similar increase in Cho signal was found in the contralateral hippocampus [59].

Alterations of Cr and Cho are not specific indicators of neuronal cell loss and if these resonances were to be included in the index used in this study for localization of the epileptogenic focus, an incorrect evaluation of the metabolite changes associated with the seizure activity may result. By comparing relative metabolite signal intensities with those observed in a reference region, located in the contralateral frontal cortex where no lesion was expected, this problem

is avoided. However, this method may also be susceptible to other variables which would alter the estimation of each metabolite, most notably signal variations due to B1 field inhomogeneities.

4.3. T2-Weighted imaging

In this study, T2-weighted image intensity did not show any significant changes. One explanation for this observation is that the ROI used for the %T2WI measurement was in the hippocampus, which does not include any cerebrospinal fluid (CSF) space or major vessels. Hyperintensities in clinical studies have been suggested to be due to either the presence of gliotic tissue, flow artifact or increased CSF space in the atrophic lesion [23]. Therefore, it is likely that the effect of gliosis alone may not have resulted in a sufficiently large change in relaxation times. MRI hyperintensity also identifies regions of necrosis and edema with acute injury after systemic injection of kainate in rats [15]. Since the model used in this study resulted in only a small lesion directly at the site of kainate injection, the damage in the selected ROIs may not have been sufficiently severe to produce significant changes.

4.4. Diffusion-weighted imaging

Decreased ADC has been measured in kainate lesions during the acute stage [24,39,46] and believed to indicate diminished extracellular space caused by cytotoxic edema. Takahashi et al. [53] found an increase in ADC with a rat stroke model in the chronic stage was related to the presence of gliosis. In this study at 1 day post-injection, there was a trend toward increased %DWI in the ipsilateral posterior hippocampus, followed by decreased %DWI after 1 week post-injection, though the change only reached significance for the ADC measurements at the 28 day time point. These findings are consistent with both of the earlier findings, suggesting that in the chronic stage of TLE, neuronal loss and gliosis result in an increase of the extracellular space. Therefore, diffusion-weighted MRI may offer a diagnostic imaging method for detection of mesial temporal sclerosis. Some improvement in the accuracy of ADC values would be gained by using a multi-point measurement, potentially offering greater significance; however, time constraints limited such a measurement in this study.

4.5. Limitations

The interpretation of ^{1}H-MRSI data is subject to several potential limitations. Firstly, changes of metabolite relaxation rates will alter signal intensities independently of changes in concentration. In this study any changes of metabolite relaxation rates have not been corrected for. For the data acquisition methods used, the results would be sensitive to changes in T2. However, in light of previous studies [47], it is felt that significant alteration of metabolite relaxation rates due to edema is unlikely due to the absence of significant intensity changes on the T2-weighted images, as well as the absence of any severe tissue necrosis. Secondly, the effect of limited sampling in MRSI results in signal contributions arising from a distributed volume of tissue which is larger than the nominal voxel volume [34]. For well-localized metabolite changes this effect will result in diminished image contrast, as well as inter-voxel contamination. For example, the ROI for posterior hippocampus was chosen to avoid the actual site of kainate injection which may have suffered tissue damage due to the injection. However, due to the close proximity of the selected posterior hippocampus ROI to the injection site, inter-voxel contamination may result in a greater decrease in the measured NAA signal. Thirdly, the resonance analyzed for NAA at 2.02 ppm also includes contributions from *N*-acetyl-aspartylglutamate (NAAG). However, any changes of NAAG would not be expected to significantly alter the NAA findings because it is present in brain only at a very low concentration. In humans the NAAG contribution has been estimated at approximately 2% of the NAA signal w43x, and HPLC measurement in rats following systemic injection of kainate found that the ratio of NAAG to NAA did not exceed 6% [40].

5. Conclusions

In this study, unilateral changes of ADC and signal intensities of NAA, Cr and Cho relative to those in an unaffected brain region, were observed with a model of temporal lobe epilepsy, with most of the changes occurring during the first 14 days. These observations, especially those for the chronic stage, may reflect morphological features and altered metabolism found in clinical cases of TLE. In addition to confirming previous reports that decreased NAA is a marker of neuronal loss, we have found increased Cho in the contralateral hippocampus, indicating changes other than neuronal loss, such as the sprouting of aberrant mossy fibers may occur. The increased ADC may indicate that diffusion-weighted imaging is useful in detecting mesial temporal sclerosis.

Acknowledgements

References

1. Amaral, DG.; Witter, MP. Hippocampal formation. In: Paxinos, G., editor. The Rat Nervous System. Academic Press; Sydney: 1995. p. 443-493.

2. Babb TL. Bilateral pathological damage in temporal lobe epilepsy. Can. J. Neurol. Sci 1991;18:645–648. [PubMed: 1777886]

3. Babb TL, Brown WJ, Pretorius J, Davenport C, Lieb JP, Crandall PH. Temporal lobe volumetric cell densities in temporal lobe epilepsy. Epilepsia 1984;25:729–740. [PubMed: 6510381]

4. Ben-Ari Y, Tremblay E, Ottersen OP. Injections of kainic acid into the amygdaloid complex of the rat: an electrographic, clinical and histological study in relation to the pathology of epilepsy. Neuroscience 1980;5:515–528. [PubMed: 6892841]

5. Ben-Ari Y, Tremblay E, Ottersen OP, Meldrum BS. The role of epileptic activity in hippocampal and 'remote' cerebral lesions induced by kainic acid. Brain Res 1980;191:79–97. [PubMed: 7378761]

6. Birken DL, and Oldendorf WH. N-acetyl-L-aspartic acid: a literature review of a compound prominent in ^{1}H-NMR spectroscopic studies of brain. Neurosci. Biobeha. Rev 1989;13:23–31.

7. Cavalheiro EA, Riche DA, Le Gal La Salle G. Long-term effects of intrahippocampal kainic acid injection in rats: a method for inducing spontaneous recurrent seizures. Electroenceph. Clin. Neurophysiol 1982;53:581–589. [PubMed: 6177503]

8. Cendes F, Andermann F, Preul MC, Arnold DL. Lateralization of temporal lobe epilepsy based on regional metabolic abnormalities in proton magnetic resonance spectroscopic images. Ann. Neurol 1994;35:211–216. [PubMed: 8109901]

9. Comair, YG.; Ng, TC.; Xue, M.; Majors, A.; Modic, M.; So, NK.; Kolem, H. Proton chemical shift imaging/spectroscopy of epilepsy; Proceedings of the Society of Magnetic Resonance in Medicine, 11th Annual Meeting; Berlin. 1992. p. 1945

10. Connelly A, Jackson GD, Duncan JS, King MD, Gadian DG. Magnetic resonance spectroscopy in temporal lobe epilepsy. Neurology 1994;44:1411–1417. [PubMed: 8058140]

11. Cronin J, Dudek FE. Chronic seizures and collateral sprouting of dentate mossy fibers after kainic acid treatment in rats. Brain Res 1988;474:181–184. [PubMed: 3214710]

12. Davenport CJ, Brown WJ, Babb TL. GABAergic neurons are spared after intrahippocampal kainate in the rat. Epilepsy Res 1990;5:28–42. [PubMed: 2303020]

13. Davenport CJ, Brown WJ, Babb TL. Sprouting of GABAergic and mossy fiber axons in dentate gyrus following intrahippocampal kainate in the rat. Exp. Neurol 1990;109:180–190. [PubMed: 1696207]

14. Duc, CO.; Meier, D.; Golay, XG.; Weber, OM.; Wieser, HG.; Boesiger, P. Investigation of temporal lobe epilepsy by quantitative 1H MRS of the hippocampus in vivo; Proceedings of the Society of Magnetic Resonance, 3rd Scientific Meeting and Exhibition; Nice: 1995. p. 1829

15. Ebisu T, Rooney WD, Graham SH, Weiner MW, Maudsley AA. *N*-acetylaspartate as an in vivo marker of neuronal viability in kainate-induced status epilepticus: 1H magnetic resonance spectroscopic imaging. J. Cereb. Blood Flow Metab 1994;14:373–382. [PubMed: 8163579]

16. Falconer MA. The pathological substrate of temporal lobe epilepsy. Guy's Hosp. Rep 1970;119:47–60. [PubMed: 4910916]

17. Fernandez EJ, Maudsley AA, Higuchi T, Weiner MW. Three dimensional 1H spectroscopic imaging of cerebral metabolites in the rat using surface coils. Magn. Reson. Imag 1992;10:965–974.

18. Gadian DG, Connelly A, Duncan JS, Cross JH, Kirkham FJ, Johnson CL, Vargha-Khadem F, Nevile BG, Jackson GD. [1]H magnetic resonance spectroscopy in the investigation of intractable epilepsy. Acta Neurol. Scand 1994;152(Suppl):116–121.

19. Guimaraes, AR.; Carr, CA.; Schwartz, P.; Prakash, MR.; Berger, UV.; Jenkins, BG.; Gonzalez, RG. Quantitative in vivo 1H MRS of excitotoxity in rats; Proceedings of the Society of Magnetic Resonance, 2nd meeting; San Francisco: 1994. p. 1413

20. Higuchi T, Fernandez EJ, Maudsley AA, Shimizu H, Weiner MW, Weinstein PR. Mapping of lactate and *N*-acetyl-l-aspartate predicts infarction during acute focal ischemia: in vivo ^{1}H magnetic resonance spectroscopy in rats. Neurosurgery 1996;38:121–130. [PubMed: 8747960]

21. Hugg JW, Laxer KD, Matson GB, Maudsley AA, Weiner MW. Neuron loss localizes human temporal lobe epilepsy by in vivo proton magnetic resonance spectroscopic imaging. Ann. Neurol 1993;34:788–794. [PubMed: 8250527]

22. Jackson GD, Berkovic SF, Tress BM, Kalnins RM, Fabinyi GC, Bladin PF. Hippocampal sclerosis can be reliably detected by magnetic resonance imaging. Neurology 1990;40:1869–1875. [PubMed: 2247236]

23. Jackson GD, Connelly A, Duncan JS, Grunewald RA, Gadian DG. Detection of hippocampal pathology in intractable partial epilepsy: increased sensitivity with quantitative magnetic resonance T2 relaxometry. Neurology 1993;43:1793–1799. [PubMed: 8414034]

24. King MD, van Bruggen N, Ahier RG, Cremer JE, Hajnal JV, Williams SR, Doran M. Diffusion-weighted imaging of kainic acid lesions in the rat brain. Magn. Reson. Med 1991;20:158–164. [PubMed: 1943656]

25. Koller KJ, Zaczek R, Coyle JT. *N*-acetyl-aspartyl-glutamate: regional levels in rat brain and the effects of brain lesions as determined by a new HPLC method. J. Neurochem 1984;43:1136–1142. [PubMed: 6470709]

26. Kuzniecky R, de la Sayette V, Ethier R, Melanson D, Andermann F, Berkovic S, Robitaille Y, Olivier A, Peters T, Feindel W. Magnetic resonance imaging in temporal lobe epilepsy: pathological correlations. Ann. Neurol 1987;22:341–347. [PubMed: 3674799]

27. Le Bihan D, Breton E, Lallemand D, Grenier P, Cabanis E, Laval-Jeantet M. MR imaging of intravoxel incoherent motions: application to diffusion and perfusion in neurologic disorders. Radiology 1986;161:401–407. [PubMed: 3763909]

28. Lees GJ. Effects of anaesthetics, anticonvulsants and glutamate antagonists on kainic acid-induced local and distal neuronal loss. J. Neurol. Sci 1992;108:221–228. [PubMed: 1517756]

29. Magloczky Z, Freund TF. Selective neuronal death in the contralateral hippocampus following unilateral kainate injections into the CA3 subfield. Neuroscience 1993;56:317–335. [PubMed: 8247263]

30. Mancuso A, Karibe H, Rooney WD, Zarow GJ, Graham SH, Weiner MW, Weinstein PR. Correlation of early reduction in the apparent diffusion coefficient of water with blood flow reduction during middle cerebral artery occlusion in rats. Magn. Reson. Med 1995;34:368–377. [PubMed: 7500876]

31. Margerison JH, Corsellis J.A. Epilepsy and the temporal lobes. A clinical. electroencephalographic and neuropathological study of the brain in epilepsy, with particular reference to the temporal lobes. Brain 1966;89:499–530. [PubMed: 5922048]

32. Mathern GW, Cifuentes F, Leite JP, Pretorius JK, Babb TL. Hippocampal EEG excitability and chronic spontaneous seizures are associated with aberrant synaptic reorganization in the rat

intrahippocampal kainate model. Electroenceph. Clin. Neurophysiol 1993;87:326–339. [PubMed: 7693444]

33. Maudsley AA, Lin E, Weiner MW. Spectroscopic imaging display and analysis. Magn. Reson. Imag 1992;10:471–485.

34. Maudsley AA, Wu Z, Meyerhoff DJ, Weiner MW. Automated processing for proton spectroscopic imaging using water reference deconvolution. Magn. Reson. Med 1994;31:589–595. [PubMed: 8057811]

35. Miller BL. A review of chemical issues in 1H NMR spectroscopy: *N*-acetyl-L-aspartate, creatine and choline. NMR Biomed 1991;4:47–52. [PubMed: 1650241]

36. Moumdjian RA, Antel JP, Yong VW. Origin of contralateral reactive gliosis in surgically injured rat cerebral cortex. Brain Res 1991;547:223–228. [PubMed: 1884197]

37. Nadler JV, Perry BW, Cotman CW. Selective reinnervation of hippocampal area CA1 and the fascia dentata after destruction of CA3-CA4 afferents with kainic acid. Brain Res 1980;182:1–9. [PubMed: 7350980]

38. Nadler JV, Perry BW, Cotman CW. Intraventricular kainic acid preferentially destroys hippocampal pyramidal cells. Nature 1978;271:676–677. [PubMed: 625338]

39. Nakasu Y, Nakasu S, Morikawa S, Uemura S, Inubushi T, Handa J. Diffusion-weighted MR in experimental sustained seizures elicited with kainic acid. Am. J. Neuroradiol 1995;16:1185–1192. [PubMed: 7677009]

40. Nimura T, Cheng FC, Graham SH, Swanson RA, Weinstein PR. Change in *N*-acetylaspartate, *N*-acetylaspartylglutamate and lactate in kainate-induced epilepsy. Soc. Neurosci. Abstr 1995;21:575.6.

41. Paxinos, G.; Watson, C. The Rat Brain in Stereotaxic Coordinates. Academic Press; Sydney: 1986.

42. Piredda S, Gale K. A crucial epileptogenic site in the deep prepiriform cortex. Nature 1985;317:623–625. [PubMed: 4058572]

43. Provencher SW. Estimation of metabolite concentration from localized in vivo proton NMR spectra. Magn. Reson. Med 1993;30:672–679. [PubMed: 8139448]

44. Pulsinelli WA, Brierley JB, Plum F. Temporal profile of neuronal damage in a model of transient forebrain ischemia. Ann. Neurol 1982;11:491–498. [PubMed: 7103425]

45. Racine RJ. Modification of seizure activity by electrical stimulation. II. Motor seizure. Electroenceph. Clin. Neurophysiol 1972;32:281–294. [PubMed: 4110397]

46. Righini A, Pierpaoli C, Alger JR, Di Chiro G. Brain parenchyma apparent diffusion coefficient alterations associated with experimental complex partial status epilepticus. Magn. Reson. Imag 1994;12:865–871.

47. Rooney WD, Ebisu T, Mancuso A, Graham S, Weiner MW, Maudsley AA. Metabolite 1H relaxation in normal and hyponatremic brain. Magn. Reson. Med 1996;35:688–696. [PubMed: 8722820]

48. Sano K, Malamud N. Clinical significance of sclerosis of the corunu ammonis. Arch. Neurol. Psychiatry 1953;70:40–53. [PubMed: 13057403]

49. Schwarcz R, Zaczek R, Coyle JT. Microinjection of kainic acid into the rat hippocampus. Eur. J. Pharmacol 1978;50:209–220. [PubMed: 689077]

50. Simmons ML, Frondoza CG, Coyle JT. Immunocytochemical localization of *N*-acetyl-aspartate with monoclonal antibodies. Neuroscience 1991;45:37–45. [PubMed: 1754068]

51. Sostman HD, Spencer DD, Gore JC, Spencer SS, Holcomb WG, Williamson PD, Prichard J, Camputaro C, Greenspan RH, Mattson RH. Preliminary observations on magnetic resonance imaging in refractory epilepsy. Magn. Reson. Imag 1984;2:301–306.

52. Sperk G, Lassmann H, Baran H, Kish SJ, Seitelberger F. Kainic acid induced seizures: neurochemical and histopathological changes. Neuroscience 1983;10:1301–1315. [PubMed: 6141539]

53. Takahashi M, Fritz-Zieroth B, Chikugo T, Ogawa H. Differentiation of chronic lesions after stroke in stroke-prone spontaneously hypertensive rats using diffusion weighted MRI. Magn. Reson. Med 1993;30:485–488. [PubMed: 8255196]

54. Tallan HH, Moore S, Stein WH. *N*-acetyl-L-aspartic acid in brain. J. Biol. Chem 1956;219:257–264. [PubMed: 13295277]

55. Tauck DL, Nadler JV. Evidence of functional mossy fiber sprouting in hippocampal formation of kainic acid-treated rats. J. Neurosci 1985;5:1016–1022. [PubMed: 3981241]

56. Urenjak J, Williams SR, Gadian DG, Noble M. Proton nuclear magnetic resonance spectroscopy unambiguously identifies different neural cell types. J. Neurosci 1993;13:981–989. [PubMed: 8441018]

57. Vance JE, Pan D, Vance DE, Campenot RB. Biosynthesis of membrane lipids in rat axons. J. Cell Biol 1991;115:1061–1068. [PubMed: 1955456]

58. Vance JE, Pan D, Campenot RB, Bussiere M, Vance DE. Evidence that the major membrane lipids, except cholesterol, are made in axons of cultured rat sympathetic neurons. J. Neurochem 1994;62:329–337. [PubMed: 8263532]

59. Vermathen, P.; Ende, G.; Laxer, KD.; Knowlton, R.; El Din, M., et al. ^{1}H-MRSI follow-up studies on epilepsy show strongly altered metabolite concentrations after surgery; Proceedings, International Society of Magnetic Resonance in Medicine; New York: 1996.

60. Wu, Z.; Maudsley, AA.; Weiner, MW. Fully automatic processing of in vivo proton spectra and spectroscopic images; Proceedings, IEEE, Nuclear Scientific Symposium and Medical Imaging Conference; San Francisco: 1993. p. 1520-1522.
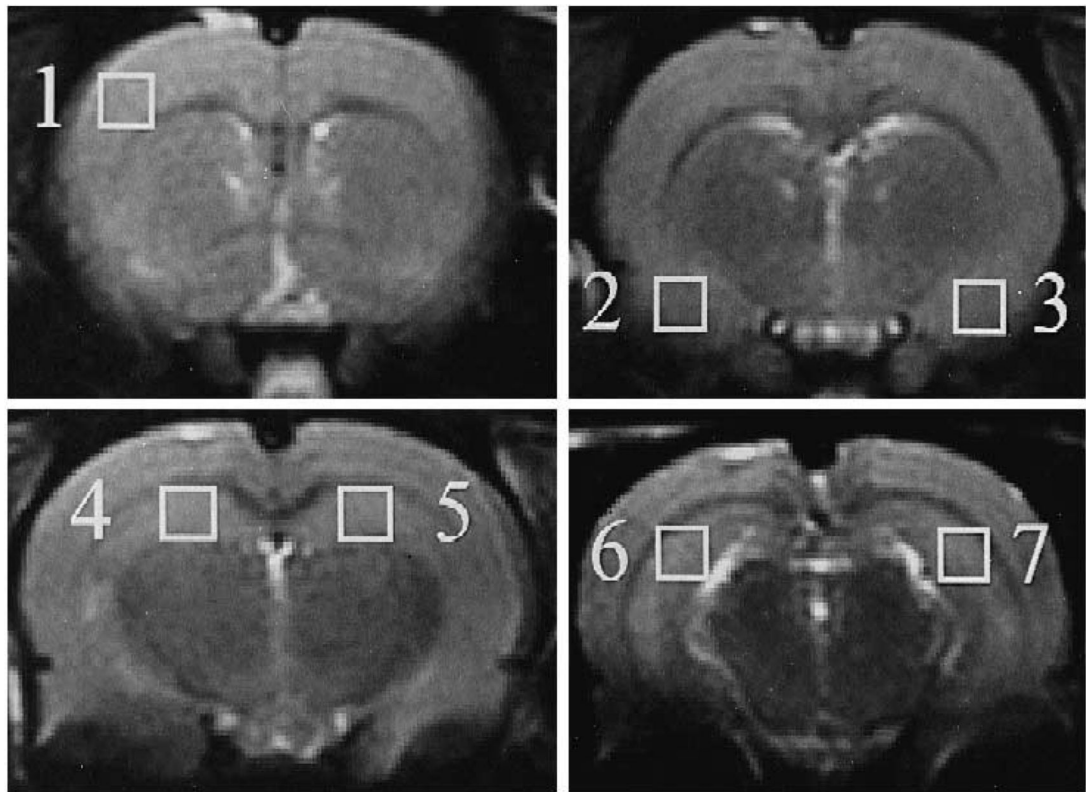
Fig. 1.
Coronal T2-weighted images showing the regions of interest selected for analysis (white squares), which are: (1) right frontal cortex; (2) right amygdala; (3) left amygdala; (4) right anterior dorsal hippocampus; (5) left anterior dorsal hippocampus; (6) right posterior dorsal hippocampus; and (7) left posterior dorsal hippocampus.
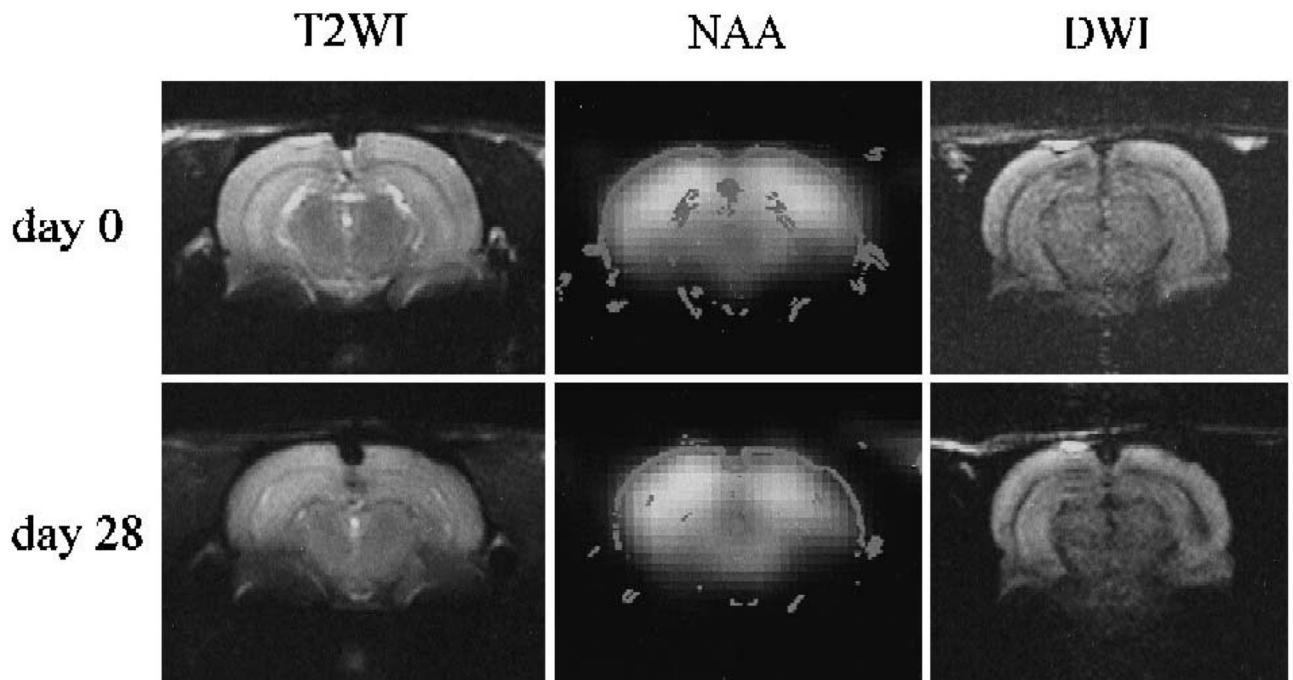
Fig. 2.
T2-Weighted images, spectroscopic images of NAA and diffusion weighted images on day 0 (upper row) and day 28 (lower row) at the slice including posterior hippocampi. Right side on the figures is left side of the rat brain.
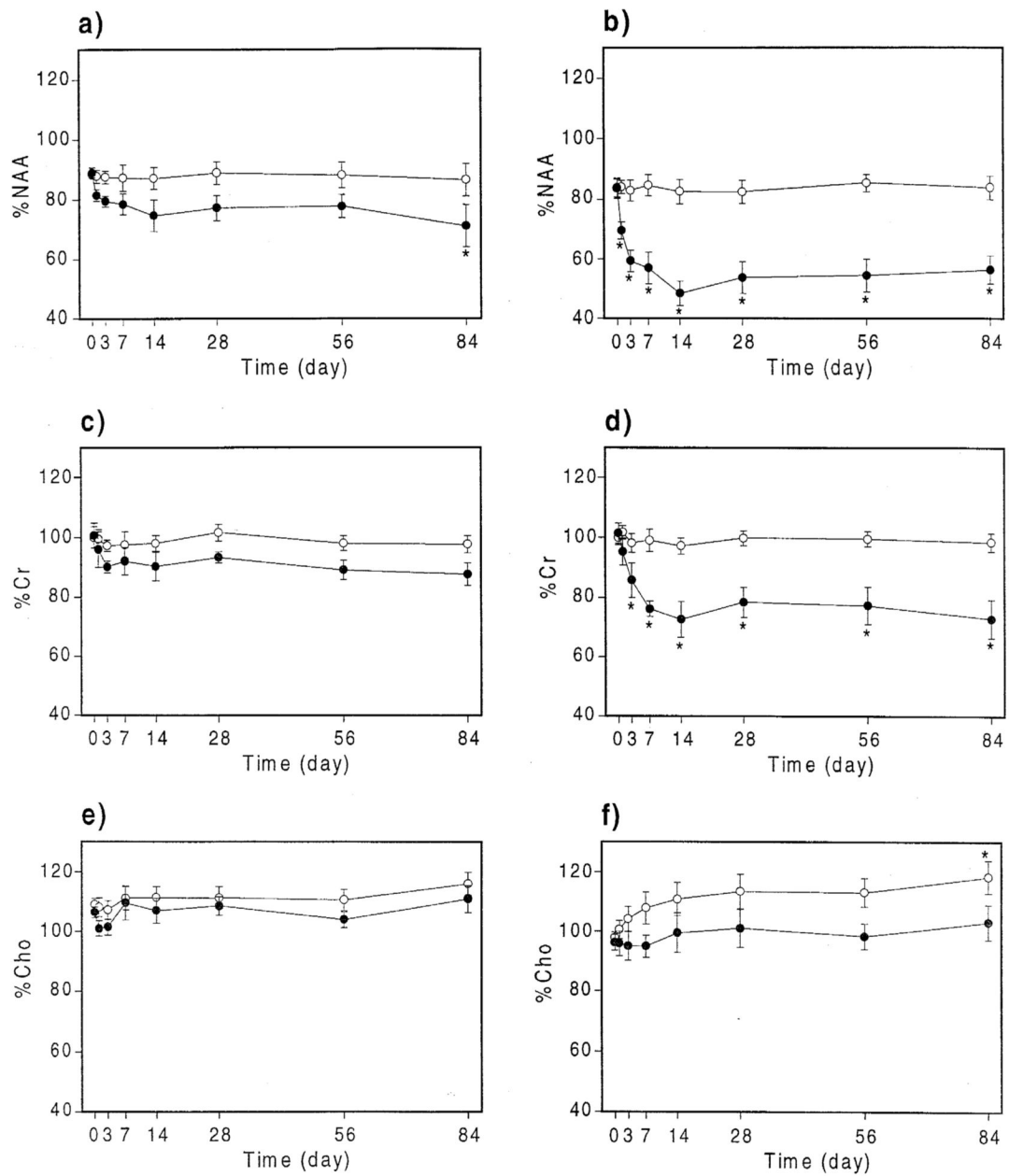
Fig. 3.
Time course of %NAA, %Cr and %Cho values for the ipsilateral (●) and contralateral (○) sides. Values are mean±standard error, with asterisks indicating significant changes compared with day 0, at *P*-0.05. Data are shown for anterior hippocampi (a, c, e) and posterior hippocampi (b, d, f).
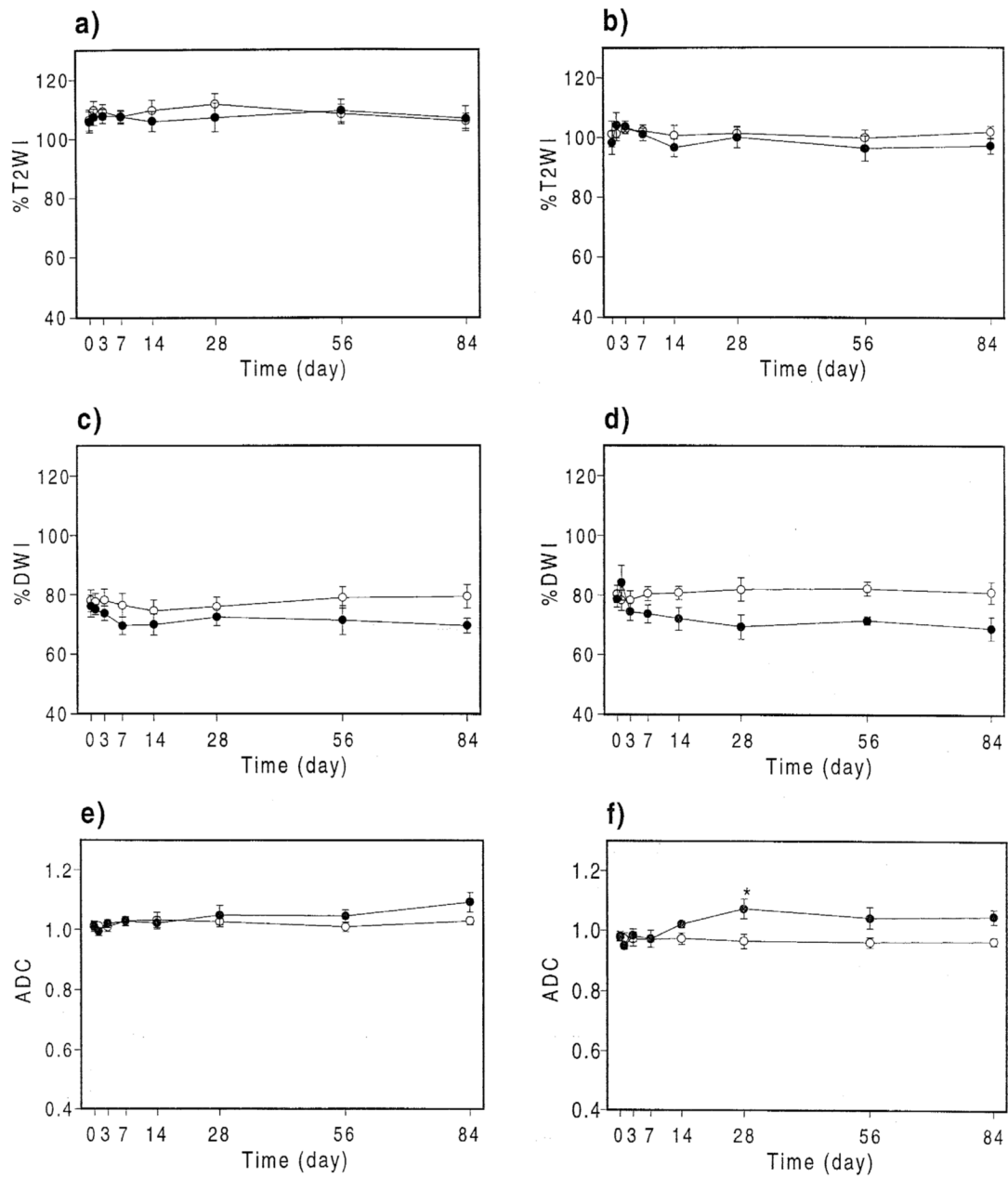
Fig. 4.
Time course of %T2WI, %DWI and ADC (10^{-3} mm^{2}s) values for the ipsilateral (●) and contralateral (○) sides. Values are mean±standard error with asterisks indicating significant changes compared with day 0 at *P*-0.05. Data are shown for anterior hippocampi (a, c, e) and posterior hippocampi (b, d, f).
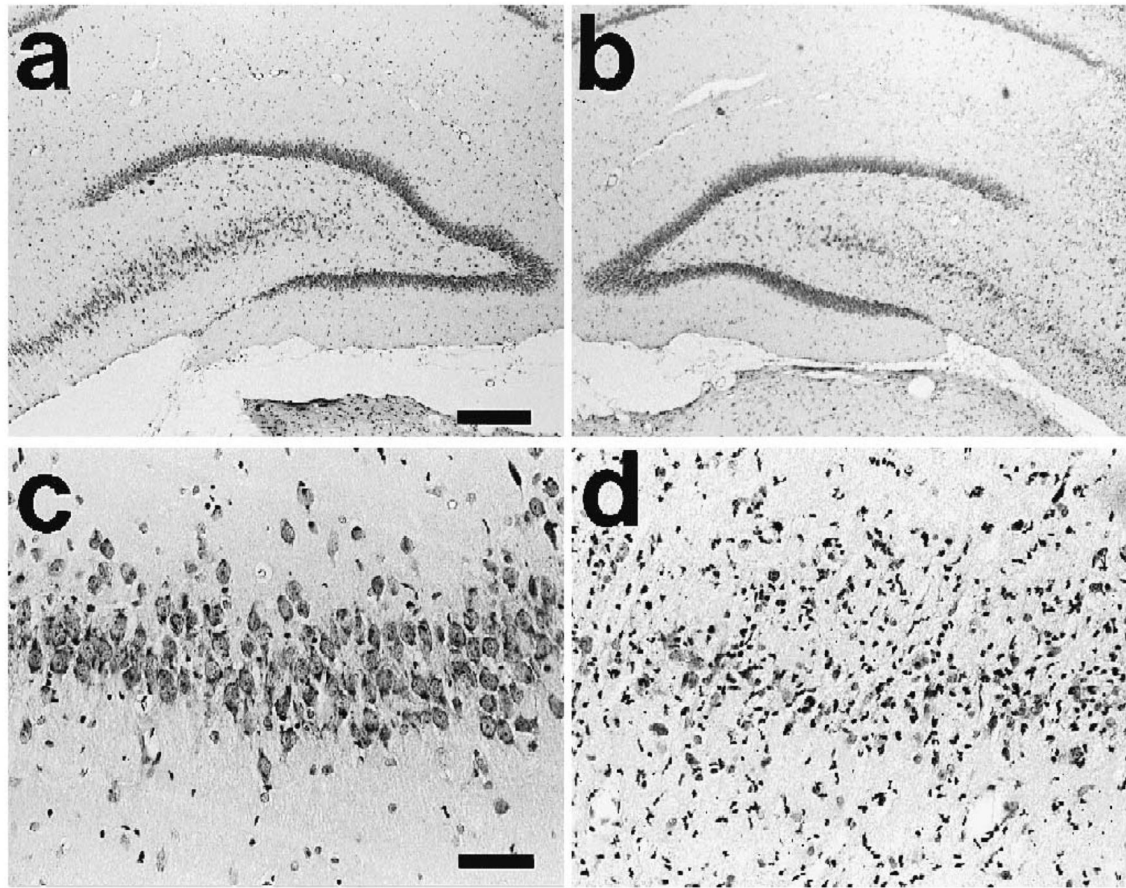
Fig. 5.
Histology example with H-E staining in the contralateral (a) and ipsilateral (b) posterior dorsal hippocampi at 28 days after kainate injection (scale bar=300 μm). Higher magnification of the contralateral (c) and ipsilateral CA3 (d) (scale bars=60 μm). The contralateral side (a, c) shows normal appearance, and the ipsilateral side (b, d) shows marked loss and gliosis in the region of CA3 and CA4.